

Magnetic reconnection and self-organization in Reversed Field Pinch laboratory plasmas

John S. Sarff¹, A. Almagri¹, J.K. Anderson¹, D.L. Brower², D. Craig¹,
B.H. Deng², D.J. Den Hartog¹, W.X. Ding², G. Fiksel¹, C.B. Forest¹,
V. Mirnov¹, S.C. Prager¹, and V. Svidzinski¹

¹Center for Magnetic Self-Organization in Laboratory and Astrophysical Plasmas and
Physics Department, University of Wisconsin, 1150 University Ave., Madison, WI 53706 USA

²Electrical Engineering Department, University of California, Los Angeles, CA 90095 USA

Abstract

Spontaneous magnetic reconnection often occurs in toroidal laboratory plasmas as a result of resistive MHD tearing instability. The interaction of these instabilities can lead to a set of magnetic self-organization phenomena, including dynamo-like effects, anomalous ion heating, anomalous momentum transport, and magnetic chaos and turbulence. A brief review of magnetic reconnection and the dynamo in reversed field pinch plasmas is presented. The reversed field pinch is a particular toroidal magnetic geometry in which the confining magnetic field is generated primarily by current in the plasma, and so magnetic self-organization is particularly strong.

1 Introduction

It has been recognized for some time that laboratory plasmas can exhibit behavior which is similar to a number of puzzling observations in astrophysical plasmas. One of the best examples is dynamo behavior, the self-generation of magnetic fields on the system size scale. In the universe, large-scale magnetic fields are observed for objects like the earth and sun, as well as for galaxies. In some laboratory plasmas, especially those for which the confining magnetic field is provided by currents flowing in the plasma itself, a large fraction of the current can be plasma self-generated, in analogy to astrophysical dynamos. Although the scales and parameters are usually very different in astrophysical and laboratory plasmas, the relative accessibility of laboratory plasmas offers a possibility to measure and understand more completely physical models invoked in the explanations of astrophysical phenomena. Greater communication and cooperation between laboratory plasma science and astrophysics will likely benefit both fields. To specifically facilitate this cooperation, a new National Science Foundation “Center for Magnetic Self-Organization of Laboratory and Astrophysical Plasmas” (CMSO) ¹ has been formed in the US to exploit and advance the physics of plasma behavior common to both environments.

This paper is a short review of magnetic reconnection and dynamo behavior in a plasma torus confined in a “reversed field pinch” (RFP) magnetic geometry (Bodin, 1990), one of the laboratory plasmas included in CMSO research. Magnetic reconnection is the root mechanism through which processes like the dynamo operate. In the RFP, spontaneous magnetic

¹ see <http://www.cmso.info> for a description of the CMSO mission and plans

reconnection occurs from both MHD tearing instability and nonlinear wave coupling, creating magnetic field, flow velocity, current density and other fluctuations in the plasma. The interaction of these fluctuations (e.g., $\langle \tilde{\mathbf{V}} \times \tilde{\mathbf{B}} \rangle_{\parallel}$ in the “alpha effect” dynamo) leads to self-organization of the mean-field plasma current and flow at the system-size scale.

Dynamo is included in this short review as an especially relevant example to *The Magnetized Plasma in Galaxy Evolution* conference theme. It is important to note, however, that other processes, such as anomalous ion heating (where ions are hotter than electrons) (Den Hartog, 2000; Reardon, 2003) and anomalous momentum transport (faster than collisional time scales) (Hansen, 2000) are observed as well. In fact, the strengths of these processes tend to track each other, as illustrated in Fig. 1. This figure shows the temporal evolution surrounding sudden onsets of increased magnetic reconnection which occur quasi-periodically in RFP plasmas. The data are for an ensemble of many similar events. Magnetic reconnection, represented in Fig. 1(a), underlies this set of phenomena which are referred to collectively as “magnetic self-organization.” The dynamo is represented in the suddenly increased magnetic flux shown in Fig. 1(b), while other magnetic self-organization phenomena are indicated in the remaining Fig. 1 panels.

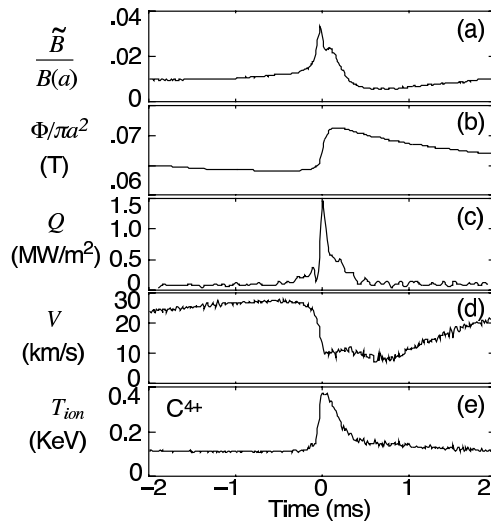


Figure 1: Magnetic self-organization processes in MST plasmas, time-resolved around bursts of increased magnetic fluctuation amplitude. (a) normalized rms fluctuation amplitude, (b) toroidal magnetic flux within the plasma torus, (c) estimate of the magnetic turbulence-induced heat flux leaving the plasma surface, (d) mean toroidal flow velocity of the plasma (in the lab frame), and (e) temperature of an impurity ion (C^{4+}).

2 Brief introduction to Reversed Field Pinch plasmas

A schematic of the RFP geometry is shown in Fig. 2. The magnetic field is generated mainly from current induced in the plasma by transformer action, although as mentioned above, some of the plasma current is sustained by dynamo action. A small portion of the magnetic field is

produced by external magnets. Except for percent-level perturbations, the plasma is axisymmetric in the toroidal direction (long way around). The magnetic field forms nested toroidal surfaces on which the plasma pressure is equilibrated. Variations depend primarily on the minor radius, crossing these surfaces. Results are shown specifically for the Madison Symmetric Torus (MST) experiment located at the University of Wisconsin-Madison (Dexter, 1991). The dimensions of the MST plasma are major radius $R = 1.5$ m and minor radius $a = 0.5$ m. Plasma currents $I_p < 0.5$ MA are produced. Other characteristic parameters for MST plasmas are listed in Table 1.

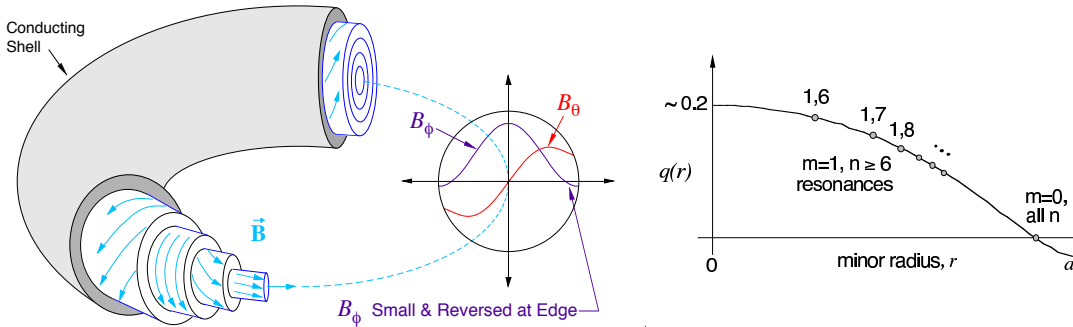


Figure 2: On the left is a cartoon schematic of the RFP magnetic geometry. B_ϕ is the toroidal component, and B_θ is the poloidal component. On the right is the radial profile $q(r) = rB_\phi/RB_\theta$, showing the resonant radii for $m = 1$ and $m = 0$ fluctuations.

Table 1: Typical plasma parameters for RFP (MST) plasmas.

Density	$n \sim 10^{19} \text{ m}^{-3}$
Electron temperature	$T_e < 1.5 \text{ keV}$
Ion temperature	$T_i \sim 0.5T_e$
Mean magnetic field	$B < 0.5 \text{ T}$
Fluctuation magnetic field	$\tilde{B}/B \sim 2\%$
Alfven timescale	$\tau_A \sim 1 \mu\text{s}$
Ion gyroradius	$\rho_i \sim 1 \text{ cm}$
Plasma beta	$\beta = W_{th}/W_{mag} \sim 0.15$
Lundquist number	$S = \tau_R/\tau_A \sim 5 \times 10^{5-6}$

In a torus, magnetic reconnection is a resonant phenomenon, occurring at locations where the magnetic perturbation's wave vector is orthogonal to the (periodic) mean field, $\mathbf{k} \cdot \mathbf{B} = 0$ (Bateman, 1978). It is convenient to express the wave vector in Fourier harmonics in the poloidal and toroidal azimuthal directions, $\mathbf{k} = m/r \hat{\theta} - n/R \hat{\phi}$. The magnetic reconnection (or tearing) resonance occurs at minor radii where

$$q(r) = \frac{rB_\phi(r)}{RB_\theta(r)} = \frac{m}{n}$$

is satisfied. Here B_ϕ and B_θ are the toroidal and poloidal mean magnetic field components

respectively, r is the minor radius, and m and n are the Fourier mode numbers. The quantity, $q(r)$, is shown in Fig. 2 for the RFP magnetic geometry. Since q decreases with minor radius, there are many radii where relatively long wavelength tearing-reconnection can occur. When the mean field equilibrium is unstable to tearing, low integer values, m, n , tend to have the largest growth rates (Robinson, 1978) and the largest fluctuation amplitudes measured in experiments.

3 Measurements of the reconnection current sheet

Measurements of the reconnection current sheet (i.e., the current density fluctuation) have been made for both an $m = 1$ mode resonant in the core of the plasma and an $m = 0$ mode resonant in the edge of the plasma. The largest $m = 1$ mode is usually the innermost resonant mode, which for MST has toroidal mode number $n = 6$. This 1,6 mode is calculated to be linearly unstable to resistive MHD tearing for the measured mean-field profiles. The instability free energy is the minor radial gradient in the current density, peaked by the tendency for induction to produce a concentration of current in the core of the plasma (Schnack, 1993). Other $m = 1$ modes are either less unstable, or grow to finite amplitude from nonlinear mode coupling. The $m = 0$ modes in the edge are calculated to be linearly stable but are observed at finite amplitude due to nonlinear coupling with the unstable $m = 1$ modes. The primary drive for MHD turbulence in the RFP is therefore $m = 1$ tearing with lowest n .

The radial profiles of the measured magnetic and current density fluctuations for the 1,6 mode are shown in Fig. 3. These measurements were made using Faraday rotation; a set of 11 parallel, elliptically polarized, far-infrared laser beams are passed through the plasma, spaced evenly across the minor radius at one toroidal azimuth (Brower, 2003). In this plane of chordal measurements, the magnetic field and current density perturbations can be reconstructed for their radial dependence (Ding, 2004). The portion of the local current and field fluctuations associated with a given n is determined by temporal cross-correlation to the n -resolved magnetic spectrum measured at the plasma surface by a toroidal array of magnetic sensors. The fluctuation in the Faraday rotation angle, $\tilde{\Psi} \approx \int n \tilde{\mathbf{B}} \cdot d\mathbf{l}$, since for $m = 1$ perturbations the density fluctuation is both small in the core and tends to average away in the chordal measurement. The finite B_r at the resonant radius implies magnetic reconnection has occurred.

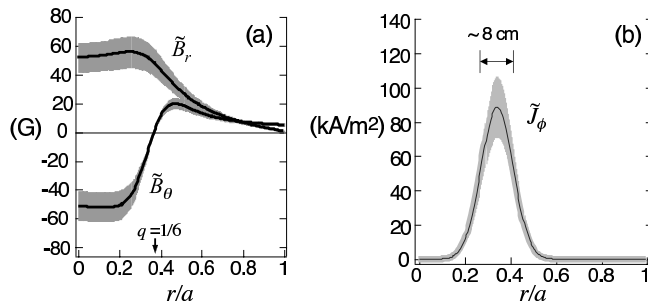


Figure 3: Faraday rotation measurements of the (a) magnetic and (b) current density fluctuations for the $m = 1, n = 6$ mode resonant in the core of MST. The shaded bands are the measurement uncertainties.

Analogous measurements to those in Fig. 3 have also been made for the $m = 0$, $n = 1$ mode resonant at the $q = 0$ radius (Crocker, 2003). In this case, small wire coils (flux loops) mounted in thin tubes are inserted radially into the plasma from the outside. The $m = 0$ resonant surface is not very deep within the plasma, making it accessible to direct probing in this way. The probe is protected by refractory materials to survive the harsh environment.

Both the core $m = 1$ and edge $m = 0$ measurements indicate that the current density fluctuation—or reconnection current sheet—is localized to a region near the resonant radius where $q = m/n$. The magnetic perturbations are more global, in agreement with MHD calculations. However, the width of both current sheets is large with respect to reconnection lengths of interest. For both the core and edge, the linear tearing layer width ($a/S^{2/5} \sim 0.2$ cm) and the electron skin depth ($c/\omega_{pe} \sim 0.5$ cm) are both small. The sheet width is closest to the ion skin depth, $c/\omega_{pi} \sim 15$ cm. There is, as yet, no complete explanation for the current sheet width, although nonlinear, resistive MHD computation produces similar widths, suggesting the current fluctuation broadens from nonlinear evolution.

4 Dynamo in the RFP

The presence of a non-inductive current drive mechanism operating in the RFP is most straightforwardly demonstrated by a measured imbalance, $E_{\parallel} \neq \eta J_{\parallel}$, in parallel Ohm's law (i.e., parallel to mean \mathbf{B}) (Anderson, Biewer et al., 2004). This is shown in Fig. 4, where E_{\parallel} and ηJ_{\parallel} are plotted versus minor radius. The current density and magnetic field are measured via reconstruction of the mean-field force-balance equilibrium, $\mathbf{J} \times \mathbf{B} = \nabla p$, using a variety of internal and external measurements (Anderson, Forest et al., 2004). The electric field results from the externally applied induction. The resistivity is taken to be the classical Spitzer value, evaluated using the measured T_e profile and $Z_{eff} = 2$ (estimated from power balance calculations). However, the neo-classical enhancement of the resistivity from electron trapping in a toroidal geometry is also included.

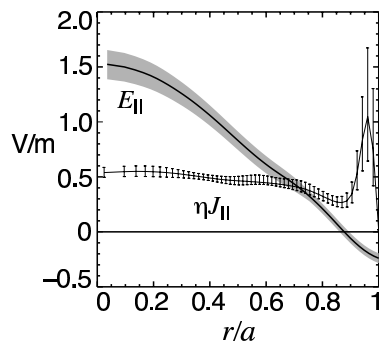


Figure 4: Radial profile of parallel Ohm's law. The imbalance $E_{\parallel} \neq \eta J_{\parallel}$ implies the presence of a turbulent dynamo.

At only one point does $E_{\parallel} = \eta J_{\parallel}$, and in particular E_{\parallel} and J_{\parallel} are antiparallel in the edge, clear evidence for a non-inductive current source. The generalized Ohm's law can be

written

$$\mathbf{E} - \eta \mathbf{J} = -\mathbf{V} \times \mathbf{B} + \frac{1}{en} \mathbf{J} \times \mathbf{B} - \frac{1}{en} \nabla p_e + \frac{m_e}{ne^2} \frac{\partial \mathbf{J}}{\partial t}$$

to expose the possible effects which would balance $E_{\parallel} - \eta J_{\parallel}$. The first term on the RHS leads to the well known ‘‘alpha effect,’’ $\langle \tilde{\mathbf{V}} \times \tilde{\mathbf{B}} \rangle_{\parallel}$ (also called the MHD dynamo). The second term on the RHS is the two-fluid Hall term which can lead to a ‘‘Hall dynamo,’’ $\langle \tilde{\mathbf{J}} \times \tilde{\mathbf{B}} \rangle_{\parallel} / en$. The tilde ‘‘~’’ over a variable represents a usually small fluctuation from the mean-field value, or specifically the non-axisymmetric component. The angle brackets indicate a spatial average over the mean-field flux surface. Dynamo effects resulting from ∇p_e have been discussed in RFP research, the so-called ‘‘kinetic dynamo’’ and ‘‘diamagnetic dynamo’’ (Ji, 1996). The electron inertia is small.

Numerous nonlinear, resistive MHD computational studies have established a standard RFP dynamo model with the balance $E_{\parallel} + \langle \tilde{\mathbf{V}} \times \tilde{\mathbf{B}} \rangle_{\parallel} = \eta J_{\parallel}$ (Schnack, 1993), but the role of two-fluid physics is only recently being investigated. Here we briefly review measurements of the MHD and Hall dynamo terms in MST, each of which are observed large enough in magnitude to balance Ohm’s law. The measurements so far do not fully span the minor radius, so the detailed balance of Ohm’s law in the experiment is not yet known. Since MHD computation had identified $\langle \tilde{\mathbf{V}} \times \tilde{\mathbf{B}} \rangle_{\parallel}$ as sufficient to balance Ohm’s law, the earliest measurements were focused on the MHD dynamo. The general approach is to measure locally, as best possible, the fluctuating $\tilde{\mathbf{V}}$ and $\tilde{\mathbf{B}}$ and correlate their cross product. This forms a direct measurement of the dynamo effect. An example of such a measurement using probes inserted in the far edge of the plasma is shown in Fig. 5 (Ji, 1996; Fontana et al., 2000). The measurement is time-resolved across events of type shown in Fig. 1 and shows that Ohm’s law is locally balanced by the MHD dynamo (i.e., the alpha effect).

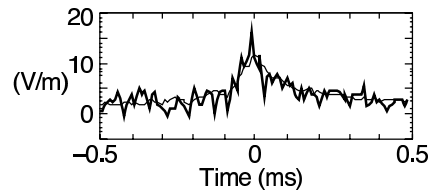


Figure 5: The thick line is a direct measurement of $-\langle \tilde{\mathbf{V}} \times \tilde{\mathbf{B}} \rangle_{\parallel}$ locally at $r/a = 0.92$ using inserted probes. The thin line is the locally measured $E_{\parallel} - \eta J_{\parallel}$. The time is relative to bursts in reconnection, as in Fig. 1. The change in J_{\parallel} is relatively small, but the plasma produces a strong inductive back reaction, causing E_{\parallel} to burst. During the burst, $-\langle \tilde{\mathbf{V}} \times \tilde{\mathbf{B}} \rangle_{\parallel} \approx E_{\parallel}$

A similar approach has been used to measure the Hall dynamo, $\langle \tilde{\mathbf{J}} \times \tilde{\mathbf{B}} \rangle_{\parallel} / en^2$. The result for the $\tilde{\mathbf{J}}$ and $\tilde{\mathbf{B}}$ data of Fig. 3 is shown in Fig. 6 (Ding, 2004). Hence a large Hall dynamo is observed for the $m = 1, n = 6$ mode in the core, concentrated near the mode-resonant surface (since $\tilde{\mathbf{J}}$ is localized there). A recent quasi-linear two-fluid theoretical calculation for tearing instability shows that the Hall dynamo can be large but localized to a narrow region around the resonant surface (Mirnov, 2003). It is therefore possible that the Hall dynamo is dominant near resonant surfaces and the MHD dynamo is dominant between surfaces. The MHD dynamo has also been measured to be large in the core of MST plasmas, but the measurement technique did not provide precise radial resolution (Den Hartog, 1999). In the

outer region, the $\langle \tilde{\mathbf{V}} \times \tilde{\mathbf{B}} \rangle_{\parallel}$ dynamo shown in Fig. 5 is observed to decrease in strength as the probes are inserted more deeply into the plasma (Fontana et al., 2000). The Hall dynamo has also been measured in edge region using probes, showing the opposite trend. Interestingly, the place where the Hall dynamo becomes large near the $m = 0$ resonant surface. These results need to be confirmed since the small but finite probe perturbations could influence the plasma.

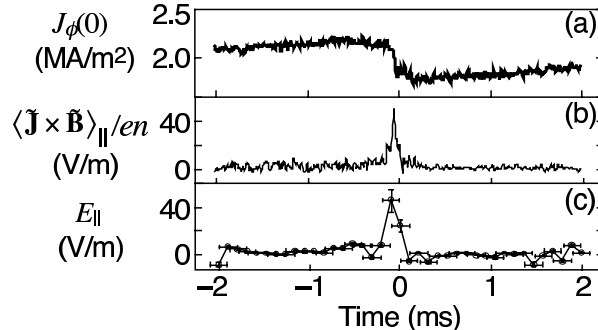


Figure 6: Hall dynamo measurement for data of Fig. 3. (a) The mean current density in the vicinity of the 1,6 resonant surface, (b) the measured Hall dynamo for the 1,6 mode, and (c) the parallel electric field. At the time of the sudden reconnection change at $t = 0$, $\langle \tilde{\mathbf{J}} \times \tilde{\mathbf{B}} \rangle_{\parallel} / en^2 \approx E_{\parallel}$. (The change in ηJ_{\parallel} is small.)

5 Summary

Magnetic reconnection resulting from MHD tearing instability and nonlinear mode coupling is observed in toroidal Reversed Field Pinch plasmas. The current sheet is localized near the mode resonant surface, but the width of the sheet is larger than linear MHD expectations. Observations of dynamo behavior are presented as an example of magnetic self-organization processes that link magnetic reconnection to large scale structure. The “alpha effect” is strong in RFP plasmas, but dynamo resulting from the Hall term $\langle \tilde{\mathbf{J}} \times \tilde{\mathbf{B}} \rangle_{\parallel} / en^2$ is also strong, implying two-fluid physics is important in the underlying magnetic reconnection.

Acknowledgments

The authors wish to thank many members of the MST research team who contributed to the results presented in this paper. This work was supported by the US Department of Energy and the National Science Foundation.

References

A somewhat dated review on the RFP is given by H.A.B. Bodin, 1990, Nucl. Fusion 9, 1717

- D.J. Den Hartog and D. Craig, 2000, *Plasma Phys. Control. Fusion Plasma Phys. Control. Fusion* 42, L47-L53
- J.C. Reardon, D. Craig, G. Fiksel, D.J. Den Hartog, 2003, S.C. Prager, *Rev. Sci. Instrum.* 74, 1892
- A.K. Hansen, A.F. Almagri, D. Craig, D.J. Den Hartog, C.C. Hegna, S.C. Prager, and J.S. Sarff, 2000, *Phys. Rev. Lett.* 85, 3408
- R.N. Dexter, D.W. Kerst, T.W. Lovell, S.C. Prager, and J.C. Sprott, 1991, *Fusion Tech.* 19, 131
- Glenn Bateman, 1978, *MHD Instabilities*, The MIT Press, Cambridge, MA
- S. Ortolani and D.D. Schnack, 1993, *Magnetohydrodynamics of Plasma Relaxation*, World Scientific Publishing, New Jersey
- D.C. Robinson, 1978, *Nucl. Fusion* 18, 939
- D.L. Brower, W.X. Ding, S.D. Terry, J.K. Anderson, T.M. Biewer, B.E. Chapman, D. Craig, C.B. Forest, S.C. Prager, and J.S. Sarff, 2003, *Rev. Sci. Instrum.* 74, 1534
- W.X. Ding, D.L. Brower, D. Craig, B.H. Deng, G. Fiksel, V. Mirnov, S.C. Prager, J.S. Sarff, and V. Svidzinski, 2004, *Phys. Rev. Lett.* 93, 045002-1
- N. Crocker, G. Fiksel, S.C. Prager, J.S. Sarff, 2003, *Phys. Rev. Lett.* 90, 035003
- J.K. Anderson, T.M. Biewer, C.B. Forest, R. O'Connell, S.C. Prager, and J.S. Sarff, 2004, *Phys. Plasmas* 11, L9
- J.K. Anderson, C.B. Forest, T.M. Biewer, J.S. Sarff, and J.C. Wright, 2004, *Nucl. Fusion* 44, 162
- H. Ji, S.C. Prager, A.F. Almagri, J.S. Sarff, Y. Yagi, Y. Hirano, K. Hattori, and H. Toyama, 1996, *Phy. Plasmas* 3, 1935
- P.W. Fontana, D.J. Den Hartog, G. Fiksel, and S.C. Prager, 2000, *Phys. Rev. Lett.* 85, 566
- V. Mirnov, C. Hegna, S. Prager, 2003, *Plasma Physics Reports (Fizika Plazmy)* 29
- D.J. Den Hartog, J.T. Chapman, D. Craig, G. Fiksel, P.W. Fontana, S.C. Prager, and J.S. Sarff, 1999, *Phys. Plasmas* 6, 1813